Received: 31 March 2021 | Revised: 9 July 2021 | Accepted: 21 August 2021

DOI: 10.1049/tje2.12078

The Journal of Engineering

The Institution of Engineering and Technology WILEY

ORIGINAL RESEARCH PAPER

Robust controller design for rotary inverted pendulum using $H\infty$ and μ-synthesis techniques

Sourav Pramanik[1] | **Sohel Anwar**[2]

[1] Mechanical Engineering, Purdue University, Indianapolis, Indiana, USA

[2] Mechanical Engineering, Purdue School of Engineering and Technology, Indianapolis, Indiana, USA

Correspondence
Sourav Pramanik, Mechanical Engineering, Purdue University, 723 W. Michigan Street, SL 260, Indianapolis, IN 46202, USA.
Email: spraman@purdue.edu

Abstract

An $H\infty$ controller is designed to control a rotary inverted pendulum in its upright equilibrium position. The key contribution of this work is a robust controller architecture design to accommodate for uncertainty in actuator model. Robust stability and performance for a given degree of actuator and measurement uncertainty is achieved using the well established techniques of μ-synthesis and $H\infty$ robust control methods. The design focuses on stabilizing an Inverted Pendulum in an upright position within a tolerable desired angle margin (α). A dynamic plant is designed based on already established theories and published papers. It is observed that the plant is completely observable for the pendulum angle and the motor arm link angle. These two signals are also measurable via encoders and is used as an input for the controller. The output of the controller is voltage actuation which drives the motor to stabilize the pendulum in an upright position ($= 0$ with $+/-$ 10 deg tolerance). A Robust Stability analysis is done along with Robust Performance, to study the stability and performance margins under modelled uncertainties. As a comparative study, a rudimentary pole placement method is also analyzed.

1 | INTRODUCTION

Rotary Inverted Pendulum is a modified version of the Pendulum on a cart. This is also known as Furuta Pendulum after its inventor Katsuhisa Furuta who invented it in 1992 at Tokyo Institute of Technology. The whole setup consists of two links attached to each other at right angle. One link is driven my a motor which in turn controls the other link (the pendulum). The pendulum has a mass attached to its tip. There are basically two objectives of the system:

- To balance the pendulum in an upright position with certain degree of tolerance from the vertical upright position which is considered as π deg. [Vertical pendulum angle (α) is measured from the downward negative y axis direction and hence the upright position is described as π deg.]
- To swing up the pendulum from its passive equilibrium position (hanging under its weight due to gravity), so that the balancing controller can balance it in the upright position.

This paper examines and studies the balancing algorithm. A robust controller to reject any disturbance at its upright equilibrium position is designed using $H\infty$ and μ-synthesis methods.

Figure 1 shows the control strategy of the rotary inverted pendulum and the highlighted portion shows the controller which we discuss. The swing up control strategy along with the switching algorithm between the swing up and the balancing controller is not discussed.

1.1 | Background

The non-linear dynamics of a Rotary Inverted Pendulum and its control in various form is a very prominent topic in research fraternity. There are numerous control schemes that are studied and published in open literature. This work references a few notable and promising algorithms. An Euler-Lagrange formalisation in an environment with external forces and friction for a double inverted pendulum is presented in [3]. The investigated properties of this work include stability of equilibrium points, a chaos of dynamics and non-minimum phase behaviour around an upper position. A lot of work has been done to implement and analyze robust control methods for rotary inverted pendulums as well. Taylor et al. [4] in general presented a novel data driven approach to control a non-linear dynamical system with actuation uncertainty. This is very close to the

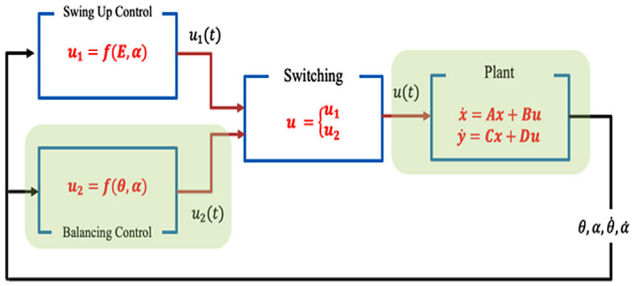

FIGURE 1 Rotary Inverted Pendulum Control Strategy. Two control action is needed—swinging up the pendulum and then balancing the pendulum. This work discusses only balancing part [1, 2]

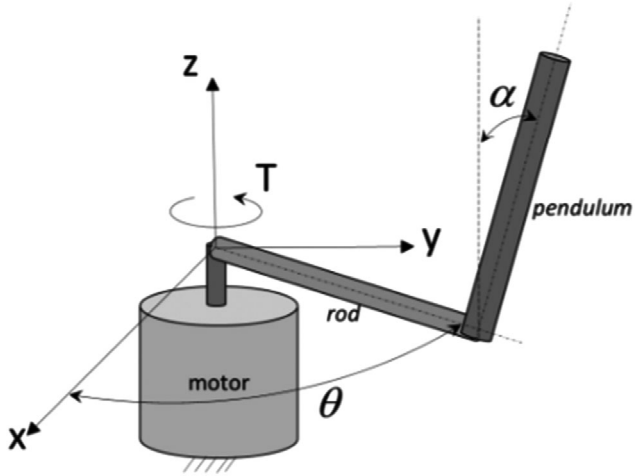

FIGURE 2 Illustration of the Dynamics of Rotary Inverted Pendulum. The horizontal and the vertical arms are connected via a 1 Degree of Freedom joint

balancing controller principle. An under-actuated cart-type inverted pendulum system with two-degree-of-freedom (2DOF) having time-varying uncertainties is studied by Sahnehsaraei et al. using approximate feedback linearization based optimal control [5]. The control law is improved with the aid of a novel adaptive approach based on an approximating function found via a multiple-crossover genetic algorithm so that the system always will be optimally robust against time-varying parametric uncertainties. Multiple robust control design methods are also studied using $H\infty$ control [6–8]. While this methods use the traditional principles of $H\infty$ controls they do not discuss the challenges associated with these methods or the robustness in handling an uncertainty level. A nice approach towards fault estimation and fault tolerant system with uncertainty and disturbance is studied by Sabbaghian et al. [9], using a polynomial based Fuzzy observer. A Programmable Logic Controller based Proportional-Integral-Derivative and Sliding mode controller scheme is discussed by Howimanpron et al. [10]. This work discussed the traditional control scheme with implementation details using a Programmable Logic Controller. A more recent method using reinforcement learning based control of a rotary inverted pendulum is designed in paper [11]. We discuss Q-Learning and Proportional-Derivative control based parameter estimation techniques. Mehedi, et al. in [12, 13] proposed two methods for order integral scheme and a 3 degree of freedom stabilization using generalized dynamic inversion control respectively. Both the papers focused more towards a generic control architecture and system selection which does not involve uncertain robust dynamic measurements. While traditional control schemes are widespread, a number of modern Fuzzy logic based architectures are also discussed a lot in literature with respect to controlling a double inverted pendulum. [14] and [15] discussed two such Fuzzy logic based control scheme respectively.

The key contribution of this paper is the design and tradeoff analysis for a robust controller structure using both $H\infty$ and μ-synthesis methods using the *MATLAB*© tool set. A number of $H\infty$ based methods are also proposed in literature, but they did not study the robustness to uncertainties in detail [16, 17]. While all these methods show very nice control structures and schemes along with stable results but a deeper study on robustness and uncertainty is not explored a lot in literature. The basic objective of this work is to understand the robustness of the system to uncertain actuator dynamics and disturbances. The challenges in handling $H\infty$ controller beyond a certain uncertainty is identified and the resolution with corresponding μ-synthesis methods are discussed. It is noted that with the μ-synthesis techniques the controller is much more robust to uncertainties. It is also noted that the tradeoff to handle uncertainties is to have a controller of higher degree which is often challenging to implement.

2 | PENDULUM DYNAMICS AND MATHEMATICAL MODELLING

Figure 2 shows the schematic of a rotary inverted pendulum. It depicts the pendulum as a lumped mass at half of the pendulum length. The pendulum is displaced with an angle α in the y-axis while the direction of θ is in the x-axis direction in this illustration. So, the mathematical model can be derived by examining the velocity of the pendulum center of mass. The following assumptions are important in modeling the system:

- The system starts in a state of equilibrium meaning that the initial conditions are assumed to be zero.
- The pendulum does not move more than a few degrees away from the vertical to satisfy a linear model.
- A small disturbance can be applied on the pendulum.

As a requirement specification, the desire is to have a quick settling time and less overshoot (*Oscillations*). The Rotary Inverted Plant model is designed based on published papers available in public domain [1, 2, 8]. There are two components for the velocity of the Pendulum lumped mass. The kinematics can be determined from Lagrange's equation,

$$\frac{d}{dt}\frac{\partial L}{\partial \dot{q}} - \frac{\partial L}{\partial q} = Q - \frac{\partial D}{\partial \dot{q}} \tag{1}$$

where, $L = T - U$, T is the Kinetic Energy, U is the Potential Energy, Q is a generalized force vector, $\frac{\partial D}{\partial q}$ represents dissipative energy from damping and q is the two-state output.

The kinetic energy of the rotary arm is defined by the rotational kinetic energy,

$$T_{arm} = \frac{1}{2} J_{arm} \dot{\theta}^2 \tag{2}$$

and the kinetic energy of the pendulum is the sum of rotational kinetic energy and translational kinetic energy,

$$T_{pend} = \frac{1}{2} J_p \dot{\alpha}^2 + \frac{1}{2} m_p \dot{r}_p^T \dot{r}_p \tag{3}$$

where r_p is the position vector of the pendulum center of mass in 3D space,

$$\boldsymbol{r_p} = \begin{bmatrix} x_p \\ y_p \\ z_p \end{bmatrix} = \begin{bmatrix} r\sin(\theta) + l_p \sin(\alpha)\cos(\theta) \\ h - l_p \cos(\alpha) \\ r\cos(\theta) - l_p \sin(\alpha)\sin(\theta) \end{bmatrix}, \tag{4}$$

$$\dot{\boldsymbol{r}}_{\boldsymbol{p}} = \begin{bmatrix} r\dot{\theta} c_\theta + l_p \dot{\alpha} c_\alpha c_\theta - l_p \dot{\theta} s_\alpha s_\theta \\ l_p \dot{\alpha} s_\alpha \\ -r\dot{\theta} s_\theta - l_p \dot{\alpha} c_\alpha s_\theta - l_p \dot{\theta} s_\alpha c_\theta \end{bmatrix} \tag{5}$$

where $c_\theta = \cos(\theta)$, $s_\theta = \sin(\theta)$, $c_\alpha = \cos(\alpha)$, and $s_\alpha = \sin(\alpha)$. Now to find T, $\dot{r}_p^{\,T} \dot{r}_p$ is expanded for the quadratics, common terms are combined and some terms are cancelled. Thus we find the energy terms as,

$$T = \frac{1}{2} J_{arm} \dot{\theta}^2 + \frac{1}{2} J_p \dot{\alpha}^2 + \frac{1}{2} m_p \left(r^2 \dot{\theta}^2 + l_p^{\,2} \dot{\theta}^2 s_\alpha^2 + 2 r l_p \dot{\theta} \dot{\alpha} c_\alpha \right) \tag{6}$$

$$U = -m_p g l_p c_\alpha \tag{7}$$

$$D = \frac{1}{2} C_{arm} \dot{\theta}^2 + \frac{1}{2} C_p \dot{\alpha}^2 \tag{8}$$

Finally using the Lagrange's equation terms and rearranging the dynamics into the original manipulator equation we write it as,

$$H(q)\ddot{q} + C(q, \dot{q})\dot{q} + G(q) = Bu \tag{9}$$

where

$$H(q) = \begin{bmatrix} J_{arm} + m_p r^2 + m_p l_p^2 s_\alpha^2 & m_p r l_p c_\alpha \\ m_p r l_p c_\alpha & J_p + m_p l_p^2 \end{bmatrix} \tag{10}$$

$$C(q, \dot{q}) = \begin{bmatrix} \frac{1}{2} m_p l_p^2 \dot{\alpha} \sin(2\alpha) + C_{arm} & \frac{1}{2} m_p l_p^2 \dot{\theta} \sin(2\alpha) \\ & -m_p r l_p \dot{\alpha} s_\alpha \\ \frac{1}{2} m_p l_p^2 \sin(2\alpha) & C_p \end{bmatrix} \tag{11}$$

$$G(q) = \begin{bmatrix} 0 \\ m_p g l s_\alpha \end{bmatrix}, B = \begin{bmatrix} 1 \\ 0 \end{bmatrix} \tag{12}$$

Note that the choice of C is not unique, and the identity $2\sin(\alpha)\cos(\alpha) = \sin(2\alpha)$ was used to determine C. This set of equations are linearized for the steady state point at upright position, for a general dynamic system,

$$\dot{x} = f(x, u), \tag{13}$$

For this system, a fixed point is an input and state combination (x^*, u^*), such that the function f evaluates to zero, that is $f(x^*, u^*) = 0$. The linearized dynamics of any system, $\dot{x} = f(x, u)$, around a fixed point can be determined by Taylor series expansion,

$$\dot{x} \approx f(x^*, u^*) + \left.\frac{\partial f}{\partial x}\right|_{x^*, u^*} (x - x^*) + \left.\frac{\partial f}{\partial u}\right|_{x^*, u^*} (u - u^*), \tag{14}$$

thus at a fixed point,

$$\dot{x} \approx \left.\frac{\partial f}{\partial x}\right|_{x^*, u^*} (x - x^*) + \left.\frac{\partial f}{\partial u}\right|_{x^*, u^*} (u - u^*), \tag{15}$$

For the general manipulator system, the dynamics, the linearized dynamics of the manipulator equation around a fixed point are given by,

$$\dot{x} = \boldsymbol{A}x + \boldsymbol{B}u, \tag{16}$$

where $\dot{x}$ is the full system state ($x = [q, \dot{q}]^T = [\theta, \alpha, \dot{\theta}, \dot{\alpha}]^T$) and $u = \tau$ is the input torque and by the first order Taylor series approximation around a fixed point ($x*, u*$), provides the A, B, C matrices as,

$$\boldsymbol{A} = \left.\frac{\partial f}{\partial x}\right|_{x = x^*, u = u^*} (x - x^*), \tag{17}$$

Therefore, it can be written as,

$$\boldsymbol{A} = \begin{bmatrix} 0 & \boldsymbol{I} \\ -\boldsymbol{H}(q)^{-1} \frac{\partial G(q)}{\partial q} & -\boldsymbol{H}(q)^{-1} \boldsymbol{C}(q, \dot{q}) \end{bmatrix}, \tag{18}$$

$$\boldsymbol{B} = \left.\frac{\partial f}{\partial u}\right|_{x = x^*, u = u^*} (x - x^*) = \begin{bmatrix} 0 \\ \boldsymbol{H}^{-1}(q) B \end{bmatrix}, \tag{19}$$

In the actual physical system the control input is not the torque, but is actually the voltage applied to the motor. The actuator dynamics must be included into the state equations since the computer does not control the motor torque directly but controls the voltage being applied to the motor. The torque generated at the arm pivot from the motor voltage, V_m, is given by,

$$\tau = \frac{\boldsymbol{K}_t (V_m - \boldsymbol{K}_m \dot{\theta})}{\boldsymbol{R}_m} \tag{20}$$

TABLE 1 Definition of Physical Parameters used in the Design

Symbol	Description	Unit	Value
K_t	Motor torque constant	$\frac{\text{Nm}}{\text{A}}$	0.00767
K_m	Back EMF constant	Vs	767
R_m	Armature resistance	Ω	2.6
K_g	System gear ratio	None	14x1
η_m	Motor efficiency	%	69%
η_g	Gearbox efficiency	%	90%
B_{eq}	Viscous damping coefficient	$\frac{\text{Nm}}{\text{s}}$	1.5e-3
J_{eq}	Moment of inertia at the load	Kg.m^2	9.31e-4

The linear dynamics of the motor can be combined with the state space system to obtain the complete dynamics, where $x = [\theta, \alpha, \dot{\theta}, \dot{\alpha}]^T$, $u = V_m$ is the input voltage. This is achieved by transforming,

$$\boldsymbol{A} \rightarrow \boldsymbol{A} - \begin{bmatrix} \boldsymbol{0} & \boldsymbol{0} & \dfrac{\boldsymbol{\mathcal{K}_t \mathcal{K}_m}}{\boldsymbol{\mathcal{R}_m}} \boldsymbol{B} & \boldsymbol{0} \end{bmatrix}, \quad B \rightarrow \frac{\mathcal{K}_t}{\mathcal{R}_m} B, \tag{21}$$

Now since we look at the upright fixed point $(0, \pi, 0, 0)^T$, the matrices A and B are populated as,

$$\mathcal{A}(3,2) = \frac{m_p{}^2 g r l_p{}^2}{J_h J_{arm} + J_p m_p r^2 + J_{arm} m_p l_p{}^2}, \tag{22}$$

$$\mathcal{A}(3,3) = \frac{-\mathcal{K}_t \mathcal{K}_m (J_p + m_p l_p{}^2)}{\mathcal{R}_m (J_h J_{arm} + J_p m_p r^2 + J_{arm} m_p l_p{}^2)} \tag{23}$$

$$\mathcal{A}(4,2) = \frac{m_p g l_p (J_{arm} + m_p r^2)}{J_h J_{arm} + J_p m_p r^2 + J_{arm} m_p l_p{}^2}, \tag{24}$$

$$\mathcal{A}(4,3) = \frac{-\mathcal{K}_t \mathcal{K}_m (m_p r l_p)}{\mathcal{R}_m (J_h J_{arm} + J_p m_p r^2 + J_{arm} m_p l_p{}^2)} \tag{25}$$

and, A(1,1), A(1,2), A(1,4), A(2,1), A(2,2), A(2,3), A(3,1), A(2,4), A(4,1), A(4,4) are all 0 and $\mathcal{A}(1,3), \mathcal{A}(2,4)$ are 1.

$$\boldsymbol{B} = \begin{bmatrix} 0 \\ 0 \\ \dfrac{\mathcal{K}_t (J_p + m_p l_p{}^2)}{\mathcal{R}_m (J_h J_{arm} + J_p m_p r^2 + J_{arm m_p l_p{}^2})} \\ \dfrac{\mathcal{K}_t (m_p r l_p)}{\mathcal{R}_m (J_h J_{arm} + J_p m_p r^2 + J_{arm m_p l_p{}^2})} \end{bmatrix} \tag{26}$$

Therefore using the physical values from Table 1, the state space form is populated as,

$$\begin{bmatrix} \dot{\theta} \\ \dot{\alpha} \\ \ddot{\theta} \\ \ddot{\alpha} \end{bmatrix} = \begin{bmatrix} 0 & 0 & 1 & 0 \\ 0 & 0 & 0 & 1 \\ 0 & 39.32 & -14.52 & 0 \\ 0 & 81.78 & -13.98 & 0 \end{bmatrix} \begin{bmatrix} \theta \\ \alpha \\ \dot{\theta} \\ \dot{\alpha} \end{bmatrix} + \begin{bmatrix} 0 \\ 0 \\ 25.54 \\ 24.59 \end{bmatrix} V_m \tag{27}$$

The Rotary Inverted Pendulum plant model design has four states, one controlled input and four outputs. All the four outputs are not measurable and so we want to do an observability test to make sure that the plant is completely state observable with the outputs which can be measured. We have two encoders to measure the pendulum angle (α) and the motor arm link angle (θ).

$$Y = \begin{bmatrix} 1 & 0 & 0 & 0 \\ 0 & 1 & 0 & 1 \end{bmatrix} \begin{bmatrix} \theta \\ \alpha \\ \dot{\theta} \\ \dot{\alpha} \end{bmatrix} + \begin{bmatrix} 0 \\ 0 \end{bmatrix} V_m \tag{28}$$

With this set of measured outputs available, we form the observability matrix which is, $[C\ CA\ CA^2\ CA^3]^T$. The matrix is full rank and hence we conclude that the system is completely state observable with the measured outputs of the pendulum angle a and motor arm link angle q. We used *MATLAB*© command $rank(obsv(A, C))$ to get the rank of the observability matrix. We also form the controlability matrix as, $[B\ AB\ A^2B\ A^3B]$. which also shows that the matrix is full rank and hence is controllable. Again, we have used *MATLAB*© command $rank(ctrb(A, B))$ to get the rank of the controllability matrix. The open loop plant has poles at $[0, -17.1209, 7.5407, -4.9398]$. It is observed that plant has a right half plane pole which makes the system unstable and hence we need to design a controller to stabilize it.

3 | $H\infty$ CONTROLLER DESIGN

Rotary Inverted Pendulum dynamical plant has 4 outputs which are the Motor Arm Link Angle (θ), Pendulum Angle (α), Motor Arm Link Velocity($\dot{\theta}$) and Pendulum Angle Velocity ($\dot{\alpha}$). The Plant is full state observable with only the Motor Arm Link Angle and the Pendulum Angle. Hence, in physical system there are only two encoders used to read these angle values and feed to the balancing controller. This work studies only the balancing controller. In this section, the $H\infty$ controller design technique is used to design a robust controller for the Rotary Inverted Pendulum. To design the controller, we first recreate the open loop plant into a weighted system dynamical plant. There is only one control input going into the plant. So, we chose a weighting transfer function for the actuator. The transfer function is chosen based on trial and error with the knowledge of bode response and requirement. An initial guess is attempted and subsequently after a few tries a satisfactory performance is achieved with the below weighted transfer function,

$$\mathcal{W}_{act} = \frac{0.002(s + 0.01)}{s + 10} \tag{29}$$

The bode magnitude response of the Actuator Weight is shown in Figure 3.

It shows that weight puts large penalty to the system at high frequency and is designed to aim for performance at low frequencies. There are two measured outputs from the plant model

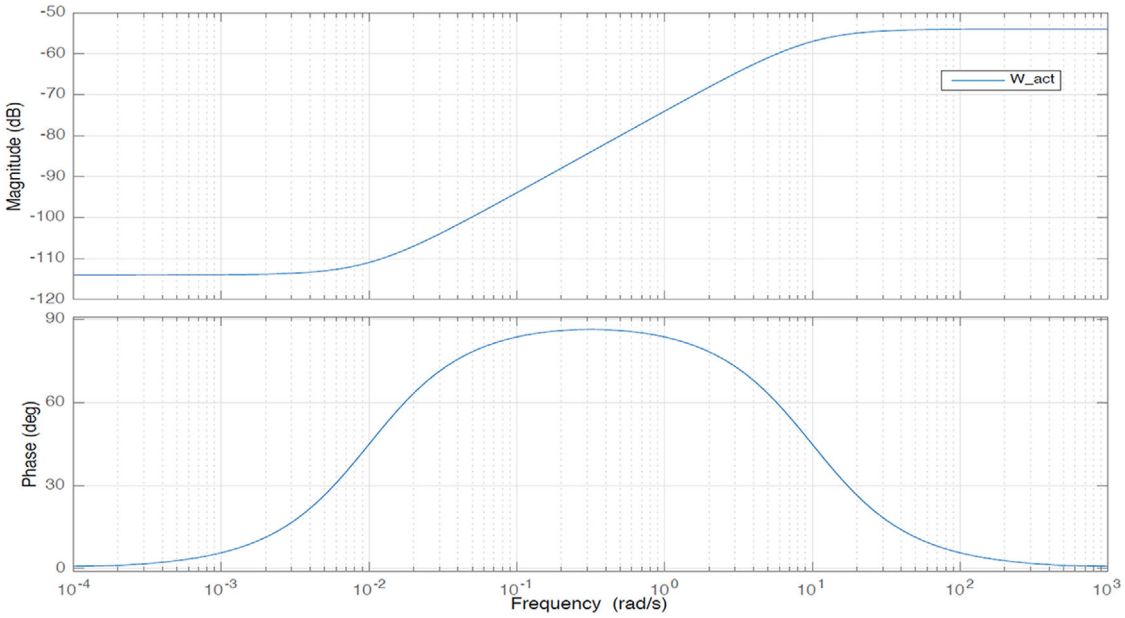

FIGURE 3 Bode Plot for Performance Weight on Actuator

which are used by the controller. Hence, we have two weighted transfer functions for the noise associated with the two measured outputs θ and α. The weights on the noise are chosen as 0.05 for the motor arm angle and **0.0275** for the pendulum angle. So, we use W_{n1} and W_{n2} as **0.05** and **0.0275**, respectively. As a performance measure we observe the pendulum arm deflection and the motor arm link angle. This are also the inputs to the controller. So, we chose two performance weight for the pendulum arm angle (α) and motor arm link angle (θ). On the performance weights, we want to aim for higher performance at high frequency since the balancing controller is not meant to stabilize the low disturbed pendulum (almost in balanced state). The selection of the performance weights is based on judicious trial and error by analyzing the bode plots. An initial weight is used with a given location of the pole and subsequently the weight is adjusted based on the result. The final satisfactory weight on the motor arm link angle and the pendulum angle is shown below,

$$W_{x1} = \frac{151.5}{s + 50.5} \tag{30}$$

$$W_{x2} = \frac{202}{s + 50.5} \tag{31}$$

The bode plot for the weights are shown in Figure 4. It has a pole at -50.5 with a DC gain of 151.5 and 202, respectively. The response shows that the magnitude is attenuated by 25 dB between a frequency of 10 rad/s to 1000 rad/s. This supports the design criteria of amplifying the response at low frequencies and attenuate it at higher frequency. The final weighted plant is designed with these chosen weights as shown in Figure 5.

The bode plot for the weights are shown in Figure 4.

3.1 | $H\infty$ controller result

With the designed plant shown in Figure 5, we run **"hinfsyn"** in matlab which gives a 7th order controller with a norm of $\gamma = 0.6951$. The poles are all on left half plane and hence depicts the system is stable. The Step response for the controller with a 1Volt input reference shows that the system response has a dominating time constant of 1 s. Some different weighting functions are also used to gain better frequency coverage, but it is observed that the trade off in $H\infty$ Closed Loop norm is not good. Some Weights in fact increased the norm to more than 1 which is not accepted for robust stability. Singular value decomposition shows a gain of **0.0476** at low frequencies and a gain of **1.2610** at high frequencies. This shows that the controller is designed to perform at high frequency. Figure 6 shows the step response of the closed loop dynamical plant running the $H\infty$ controller set up as per Figure 5.

4 | $H\infty$ CONTROLLER WITH ACTUATOR UNCERTAINTY

Now, with the closed loop plant created with the $H\infty$ Controller in place, it is required to formulate the actuator dynamics which is going to actuate the controlled input into the plant. The control architecture for the Weighted Plant model with Actuator Dynamic is shown in Figure 7. We create the actuator dynamics given in Equation (32),

$$actnom = \frac{30}{s + 30} \tag{32}$$

The actuator dynamics is a simple transfer function which feeds in the controlled input to the plant model. The bode

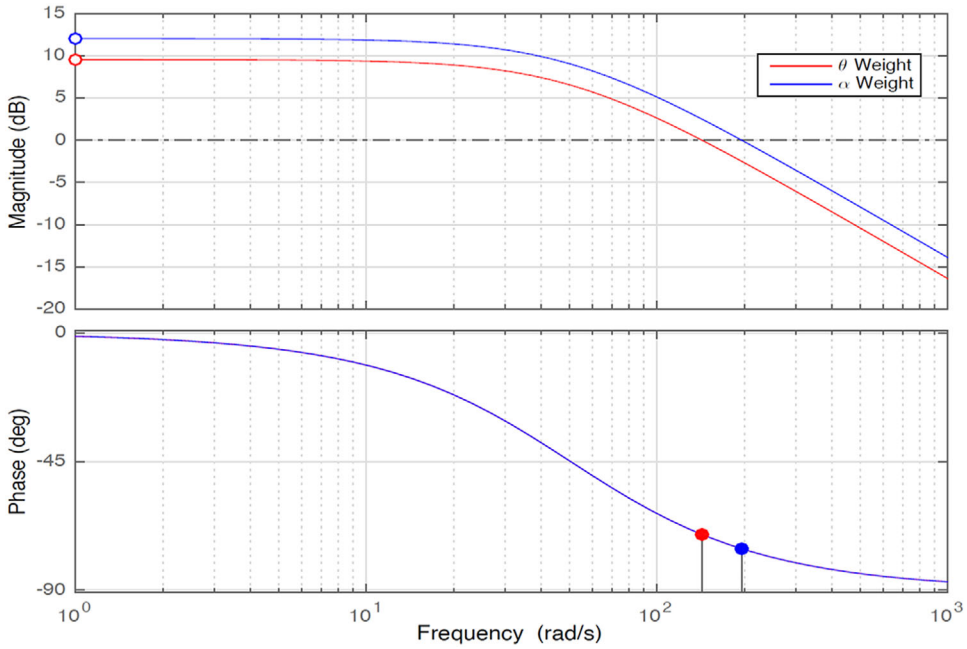

FIGURE 4 Bode Plot for Performance Weight on θ and α

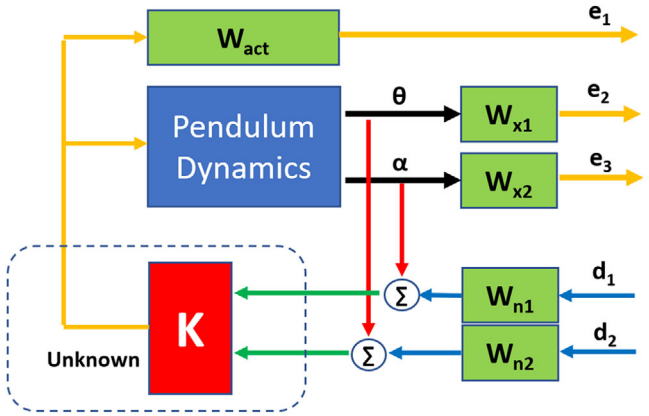

FIGURE 5 Modified weighted plant for $H\infty$ controller

response is so chosen as to make the dynamics more responsive at low frequencies for better practical hardware design. The next control design methods will include this actuator dynamics at all cases.

4.1 | $H\infty$ controller with actuator model

In this section we use $H\infty$ method to design the controller with the actuator model in place. We get a eighth order controller in *MATLAB*© using **"hinfsyn"** and a norm of $\gamma = 0.7108$. Though a stable controlled operation is achieved, the order of the controller is quite high. This will challenge the practical design of the controller. It is not impossible to design a higher order controller but will involve critical analysis in the design process and verification. This is a tradeoff which is often needed to be addressed in the design process of complex robust system with uncertainties. We notice that the $H\infty$ norm is increased slightly which is because of the actuator dynamics. The step response of the system with the actuator model is shown in Figure 8. The plots show that the actuator is able to meet the desired response and performance. Singular value decomposition shows a gain of **0.0294** at low frequencies and a gain of **0.4356** at high frequencies. This also indicates a better performance at high frequency.

4.2 | Actuator uncertain dynamics—$H\infty$ controller

Next, we involve uncertainties into the actuator model. We create an uncertain dynamics in to the actuator model. We chose a weight for the uncertainty as given by Equation (33),

$$actnom = \frac{10(s+10)}{s+500} \tag{33}$$

We used a 20% uncertainty at low frequencies which increases significantly at higher frequency saturating around 500 rad/s. The uncertain Linear Time Invariant dynamic model is created in matlab by using **[unc = ultidyn('unc', [11])** and **actmod = actnom*(1+W_{unc}*unc)]**. We created the Closed Loop Plant with this uncertain actuator dynamics, $H\infty$ controller **K** obtained above and the Open Loop Plant. The poles are all on Left Half Plane and hence depicts the system is stable. Figure 9 shows the step response for this plant with the $H\infty$ controller. It shows that the plant is not stable for some uncertainties. Using *MATLAB*© tool set to analyse the Robust Stability and Robust Performance we found that the lower bound on the

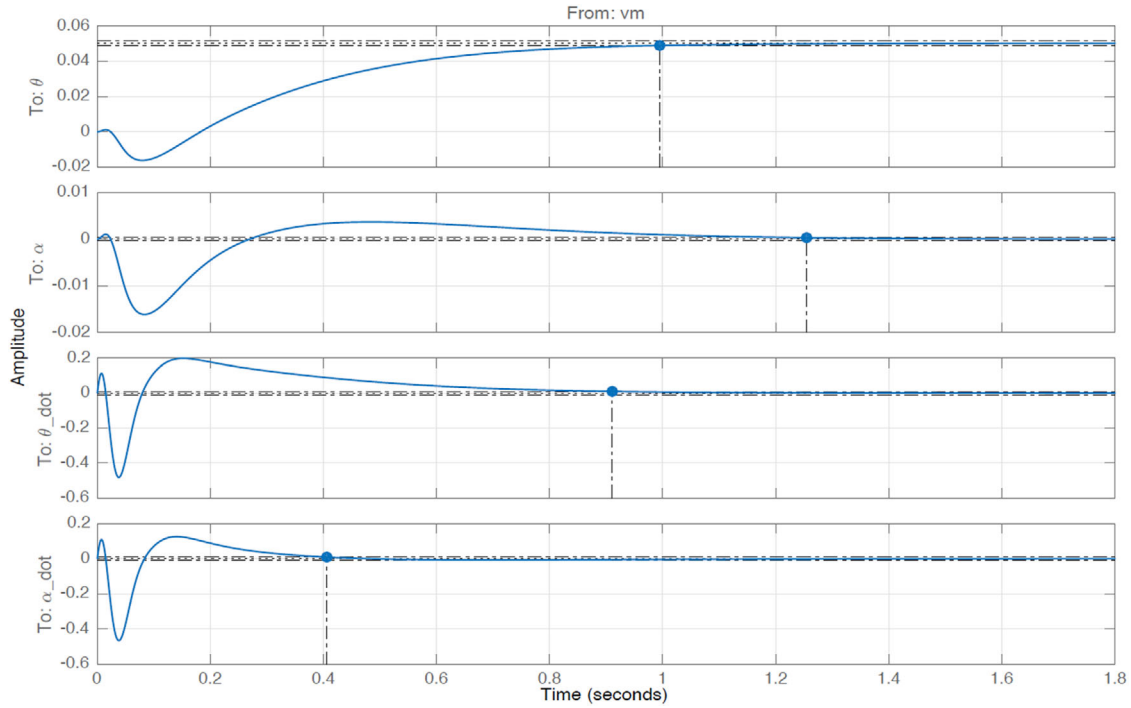

FIGURE 6 Step Response of the Closed Loop Plant with $H\infty$ Controller

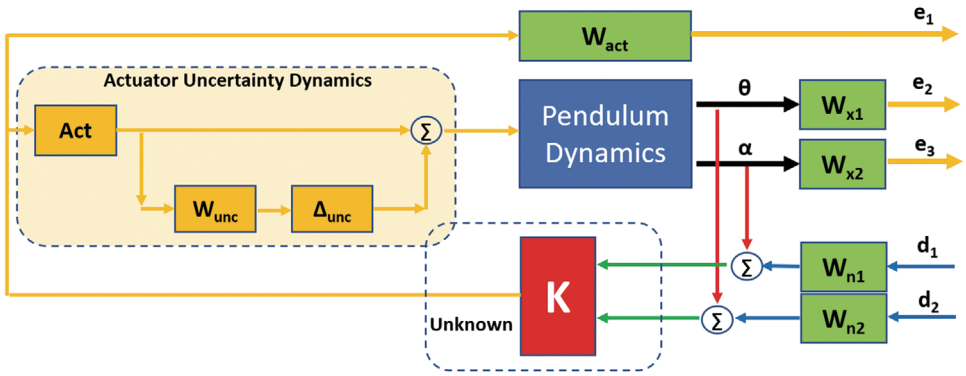

FIGURE 7 Modified weighted plant for $H\infty$ controller with Actuator Uncertainty Dynamics

stability margin is 0.1541 and the lower bound on the performance margin is **0.1431**. This shows that the system is not robust stable or achieve robust performance.

4.3 | Actuator uncertain dynamics—μ-synthesis

Next we use the μ-synthesis tool to design the controller for the uncertain plant. With the same uncertain plant with a modelled 20% uncertainty at low frequency on the actuator model we get a nineteenth order controller by the μ-synthesis tool in *MATLAB*© (dksyn). The controller achieved a $\gamma = 0.9263$. The closed loop step response of the system with the controller generated using μ-synthesis is shown in Figure 10. The singular values are shown in Figure 11. Using *MATLAB*© tool set to analyze the Robust Stability and Robust Performance we found that the lower bound on the stability margin is 1.2910 and the lower bound on the performance margin is **0.7244**. This shows that the system is robustly stable to modelled uncertainties but is does not achieve robust performance to uncertainties since the lower bound is less than 1. Moreover, the order of the controller generated is too high to implement. This is often a challenge in controller design with robust methods. The robust performance report from *MATLAB*© is shown below, *ROBUST STABILITY REPORT = Uncertain system is robustly stable to modeled uncertainty. It can tolerate up to 129% of the modeled uncertainty. A destabilizing combination of 129% of the modeled uncertainty was found. This combination causes an instability at 113 rad/s. Sensitivity with respect to the uncertain element is: unc is 100%. Increasing unc by 25% leads to a 25% decrease in the margin.*

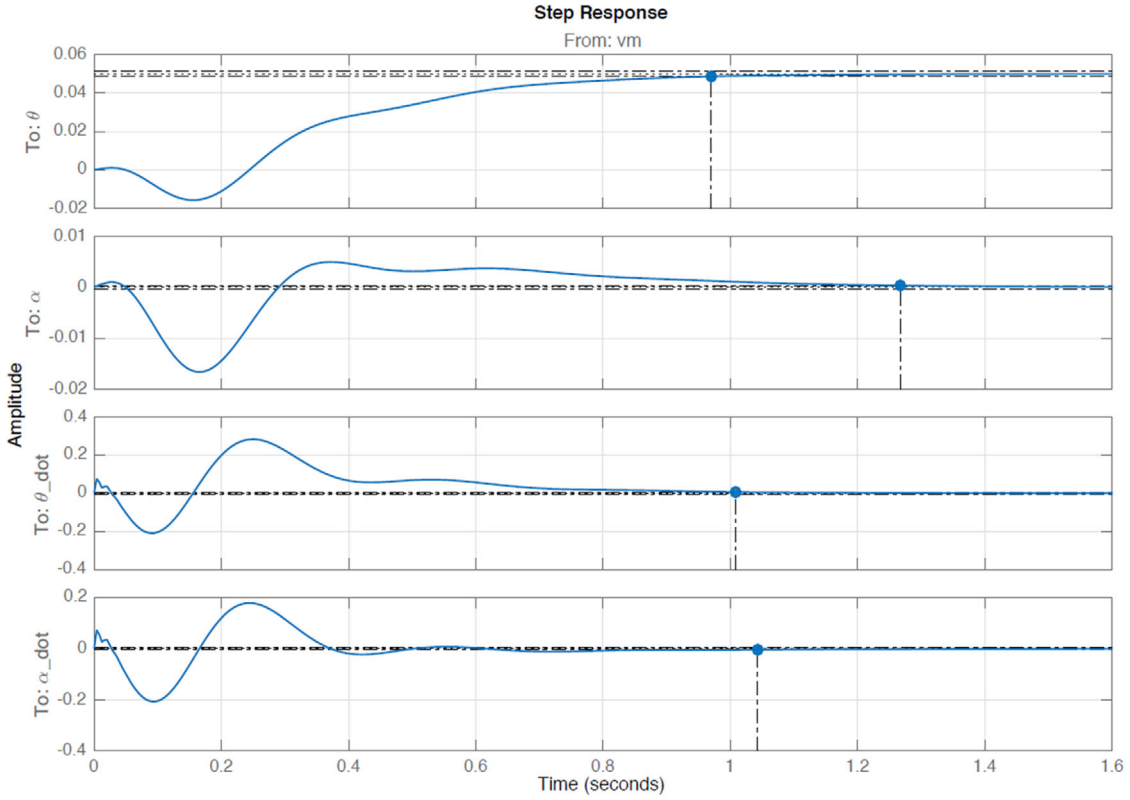

FIGURE 8 Step Response of the Closed Loop Plant using Actuator Model

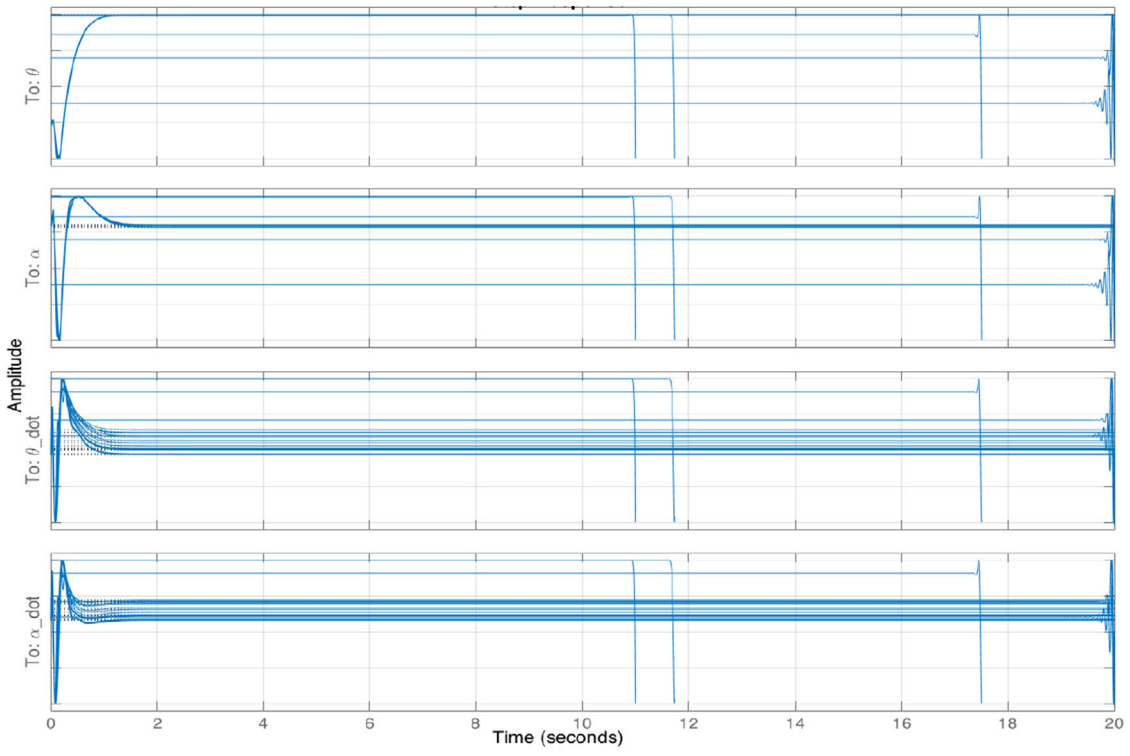

FIGURE 9 Step Response of the Closed Loop Plant using the Actuator Model Uncertainty

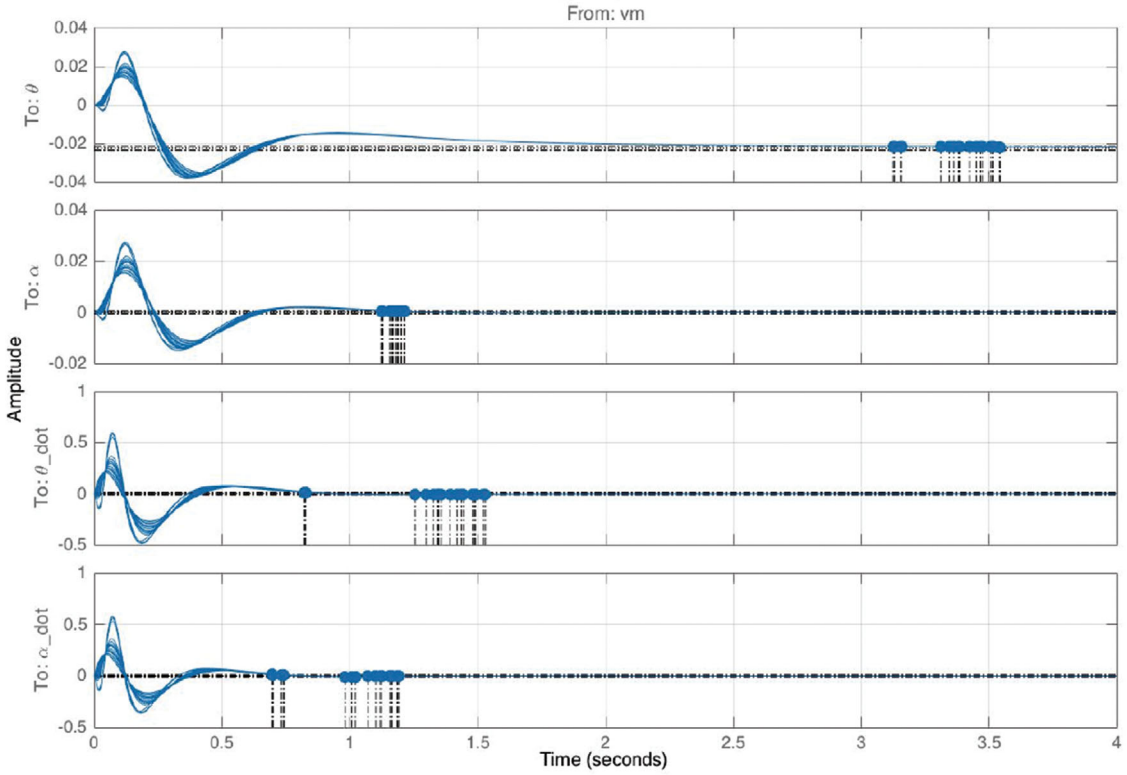

FIGURE 10 Step Response of the Closed Loop Plant with Actuator Uncertainties using μ-synthesis

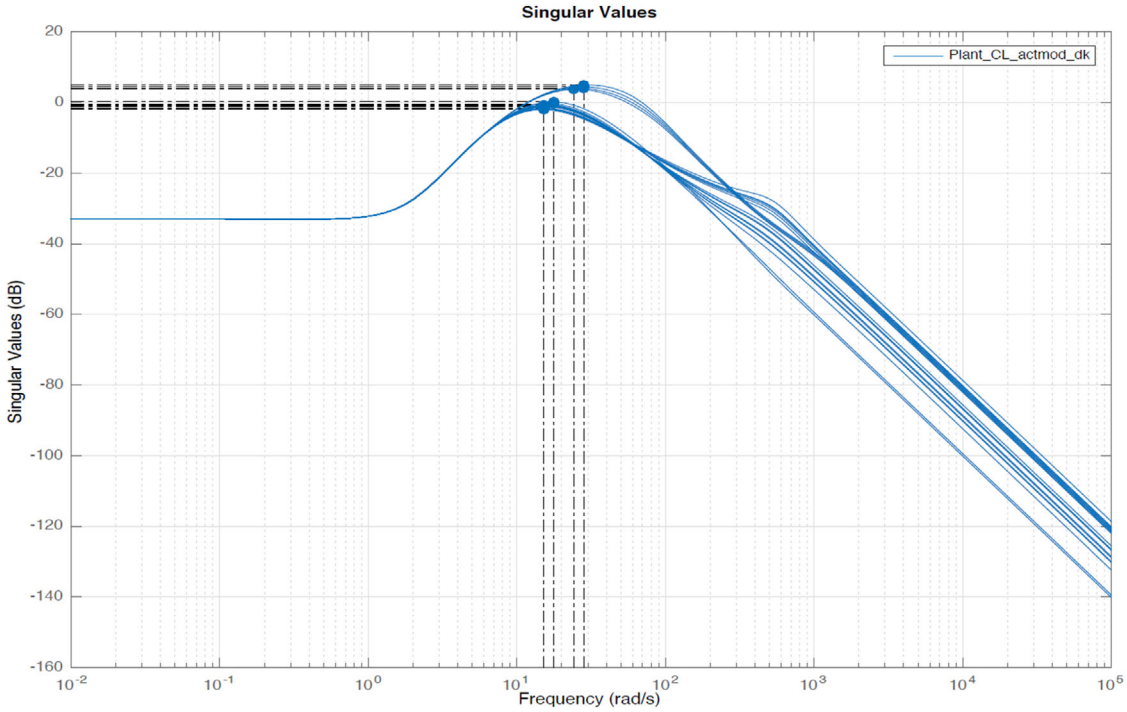

FIGURE 11 Singular Values of the Closed Loop Plant with Actuator Uncertainties—μ-synthesis

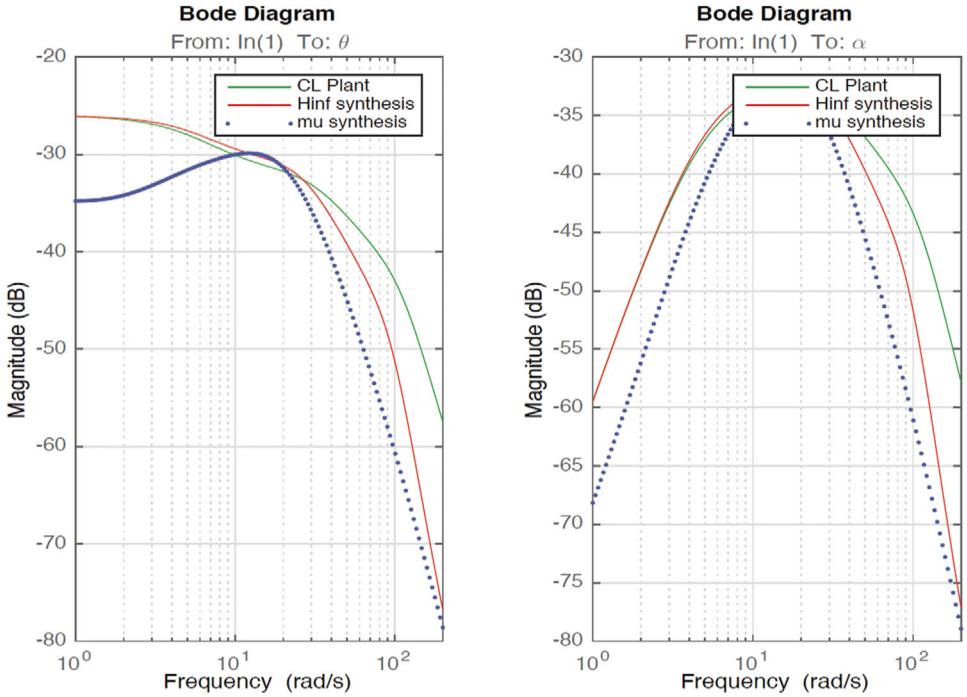

FIGURE 12 Bode Magnitude Response—$H\infty$ with Uncertainty and μ-synthesis with uncertainty

Robust Performance Report = Uncertain system does not achieve performance robustness to modeled uncertainty. The tradeoff of model uncertainty and system gain is balanced at a level of 72.4% of the modeled uncertainty. A model uncertainty of 72.4% can lead to input/output gain of 1.38 at 20.6 rad/s. Sensitivity with respect to the uncertain elements are: unc is 64%. Increasing unc by 25% leads to a 16% decrease in the margin.

4.4 | Uncertainty dynamics—μ-synthesis with reduced uncertainty levels

Since the above controller is not able to meet the modelled uncertainty level, we reduced the uncertainty to 8% which gives a lower bound on the performance margin as **1.0723**. This indicates that the desired performance robustness is achieved at the described uncertainty level. In addition, the system also gives a lower bound on the stability margin as **1.9114** and hence the system is also robust stable to modelled uncertainty. In addition to this, the controller order is also reduced to eighth which makes it easier to practically implement. The robust performance report from *MATLAB*© is shown below,

ROBUST STABILITY REPORT = Uncertain system is robustly stable to modeled uncertainty. It can tolerate up to 191% of the modeled uncertainty. A destabilizing combination of 191% of the modeled uncertainty was found. This combination causes an instability at 91.8 rad/s. Sensitivity with respect to the uncertain element is: unc is 100%. Increasing unc by 25% leads to a 25% decrease in the margin.

Robust Performance Report = Uncertain system achieves performance robustness to modeled uncertainty. The tradeoff of model uncertainty and system gain is balanced at a level of 107% of the modeled uncertainty. A model uncertainty of 107% can lead to input/output gain of 0.933 at 26.7 rad/s. Sensitivity with respect to the uncertain elements are: unc is 61%. Increasing unc by 25% leads to a 15% decrease in the margin.

Obviously, as expected the γ value of the μ-synthesis controller decreased to $\gamma = 0.7780$. The poles are all on left half plane and hence depicts the system is stable. Figure 12 shows the bode magnitude response of all the Closed Loop Plants including $H\infty$ and $\mu - synthesis$ methods with uncertainty. Figure 13 shows randomly plotted 50 samples each from the $\mu - synthesis$ controller and $H\infty$ controller for both 20% and 8% uncertainty. It is clearly visible that the robust performance is not achieved with 20% uncertainty and there are large swings in control output from the desired response.

5 | POLE PLACEMENT METHOD

As a comparison to the robust controller structure, a simple pole placement technique is used to compare the difference in performance. A set of four poles are used in the design. The poles are chosen based on trial and error methodology by analyzing the system performance. The poles used in this work are **-4.24+12.63i, -4.24-12.63i, -6.26+4.14i, -6.26-4.14i**. Using, Ackerman's technique, the controller gains are obtained by, **K=acker(A,B,P)** in *MATLAB*©. Matrices A and B are the state and the input matrices, where P is the set of desired poles. Using this we get the controller gains as, $\mathbf{K} = [-8.9144, 26.4116, -2.9755, 3.3539]^T$. Figure 14 shows the response of the system using 4 sets of poles placed in the

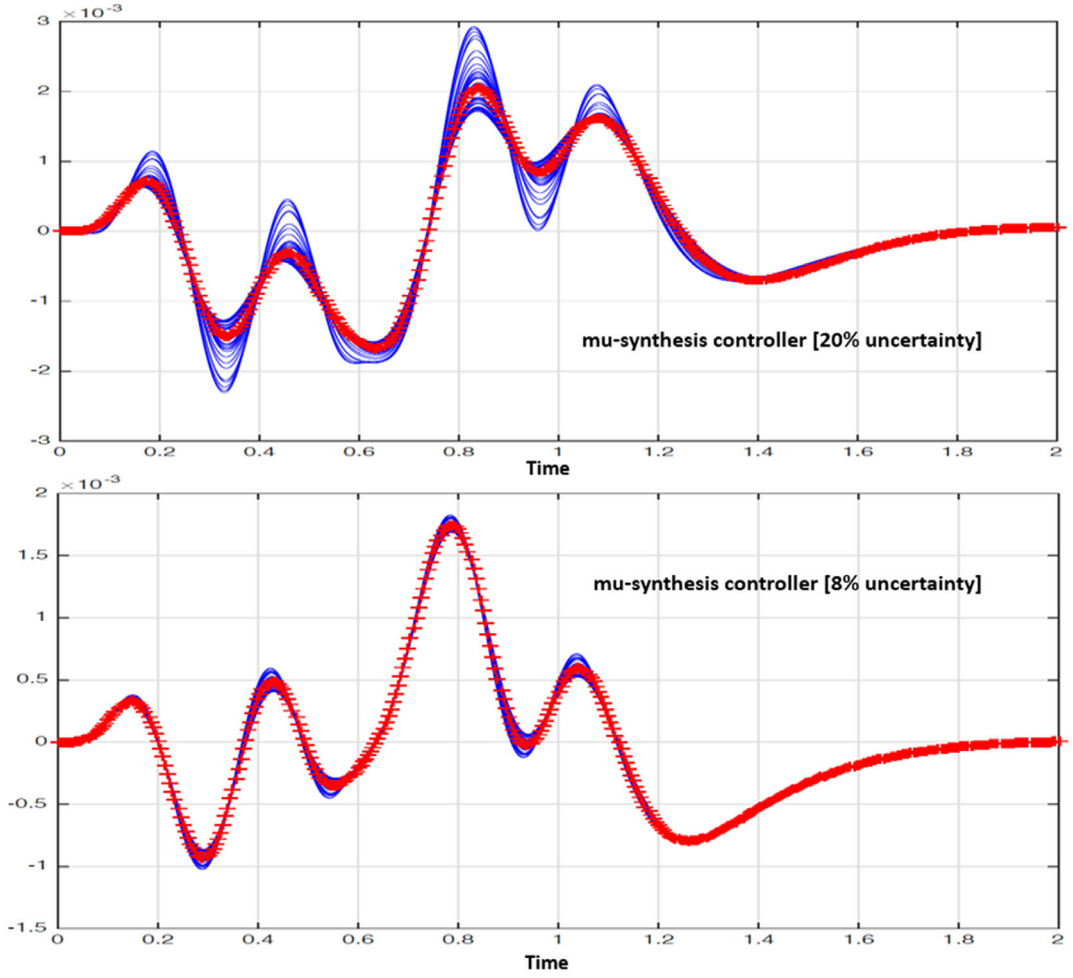

FIGURE 13 50 random Samples from μ-Synthesis Controller with 20% and 8% uncertainty

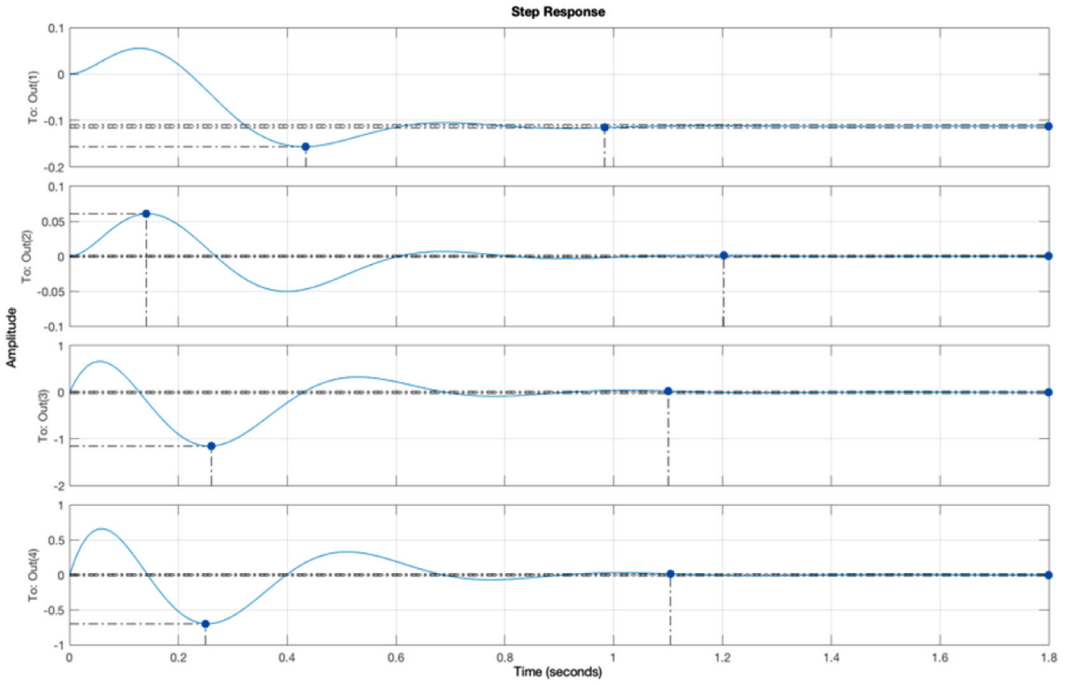

FIGURE 14 Response of the system using the pole placement method—Ackerman's Formula

closed loop feedback system using the Ackerman's formula in *MATLAB©*.

Obviously, there is no way we can have robustness analyzed for uncertainties with this structure. Though the step response shows a well-behaved response to unit step input, the performance to disturbance rejection due to uncertainties cannot be accessed with this architecture.

6 | CONCLUSION

It is seen that the $H\infty$ controller shows good response but stability and performance margins are not met, at modelled 20% uncertainty. Even though we do get an $H\infty$ norm of less than 1, the margins are not met and hence the design is not robust. With the μ-synthesis scheme at 20% modelled uncertainty the Stability specifications are met but the performance margin is not achieved. In fact the system shows to diverge to instability for some uncertain input range. Next we reduce the uncertainty to 8% and with this modelled uncertainty the design achieves both robust stability and performance margins. We achieved in designing a robust controller with modelled uncertainties using the μ-synthesis technique in *MATLAB©*. The focus was only on the balancing controller for the pendulum in the upright position. Future work would be to analyse the swing up controller as well.

CONFLICT OF INTEREST

The authors have declared no conflict of interest.

ORCID

Sourav Pramanik https://orcid.org/0000-0002-5380-0058

REFERENCES

1. Wiki, Furuta Pendulum. https://en.wikipedia.org/wiki/Furuta_pendulum. Accessed 20 October 2020
2. Ratiroch, A., Anabuki, P., Hirata, H.: Self-tuning control for rotational inverted pendulum by eigenvalue approach. Proceedings of TENCON, D, pp. 542–545. Chiang Mai, Thailand (2004)
3. Andrzejewski, K., Czyniewski, M., Zielonka, M., angowski, R., Zubowicz, T.: A comprehensive approach to double inverted pendulum modelling. Arch. Control Sci. 29(3), (2019) https://doi.org/10.24425/acs.2019.130201
4. Taylor, A.J., Dorobantu, V.D., Dean, S., Recht, B., Yue, Y., Ames, A.D.: Towards robust data-driven control synthesis for nonlinear systems with actuation uncertainty, arXiv:2011.10730v2
5. Sahnehsaraei, M.A., Mahmoodabadi, M.J.: Approximate feedback linearization based optimal robust control for an inverted pendulum system with time-varying uncertainties. Int. J. Dyn. Control 9(1), 160–172 (2021). https://doi.org/10.1007/s40435-020-00651-w
6. Silva, L.F.V., Cordeiro, T.D., de Araújo, Í.B.Q., Savino, H.J.: Robust control design for rotary inverted pendulum. Sociedade Brasileira de Automatica 2(1) (2020). https://doi.org/10.48011/asba.v2i1.1610
7. Kumar, M.A., Kanthalakshmi, S.: H$^{\infty}$ tracking control for an inverted pendulum. J. Vib. Control 24(16), 3515–3524 (2018). https://doi.org/10.1177/1077546317750977
8. Sanjeewa, S.D.A., Parnichkun, M.: Control of rotary double inverted pendulum system using mixed sensitivity $H\infty$ controller. Int. J. Adv. Rob. Syst. 16(2) (2019) https://doi.org/10.1177/1729881419833273
9. Sabbaghian, F., Farrokhi, M.: Polynomial Fuzzy Observer-based Integrated Fault Estimation and Fault Tolerant Control with Uncertainty and Disturbance. IEEE Trans. Fuzzy Syst. 1–1 (2021). https://doi.org/10.1109/tfuzz.2020.3048505
10. Howimanporn, S., Chookaew, S., Silawatchananai, C.: "Comparison between PID and Sliding Mode Controllers for Rotary Inverted Pendulum Using PLC," 2020 4th International Conference on Automation, Control and Robots (ICACR), pp. 122–126. Rome, Italy (2020). https://doi.org/10.1109/ICACR51161.2020.9265510
11. Gil, G.P., Yu, W., Sossa, H.: Reinforcement learning compensation based PD control for a double inverted pendulum. IEEE Lat. Am. Trans. 17(02), 323–329 (2019). https://doi.org/10.1109/tla.2019.8863179
12. Mehedi, I.M., Al-Saggaf, U.M., Mansouri, R., Bettayeb, M.: Stabilization of a double inverted rotary pendulum through fractional order integral control scheme. Int. J. Adv. Rob. Syst. 16(4), 172988141984674 (2019). https://doi.org/10.1177/1729881419846741
13. Mehedi, I.M., Ansari, U., AL-Saggaf, U.M.: Three degrees of freedom rotary double inverted pendulum stabilization by using robust generalized dynamic inversion control: Design and experiments. J. Vib. Control 26(23–24), 2174–2184 (2020). https://doi.org/10.1177/1077546320915333
14. Mohan, V., Rani, A., Singh, V.: Robust adaptive fuzzy controller applied to double inverted pendulum. J. Intell. Fuzzy Syst. 32(5) (2017) https://doi.org/10.3233/JIFS-169301
15. Sun, Z., Wang, N., Bi, Y.: Type-1/type-2 fuzzy logic systems optimization with RNA genetic algorithm for double inverted pendulum. Appl. Math. Modell. 39(1), 70–85 (2015). https://doi.org/10.1016/j.apm.2014.04.035
16. Sanjeewa, S.D.A., Parnichkun, M.: Control of rotary double inverted pendulum system using mixed sensitivity H∞ controller. Int. J. Adv. Rob. Syst. 16(2), 172988141983327 (2019). https://doi.org/10.1177/1729881419833273
17. Cheang, S.U., Chen, W.J.: "Stabilizing control of an inverted pendulum system based on H/sub /spl infin// loop shaping design procedure," Proceedings of the 3rd World Congress on Intelligent Control and Automation (Cat. No. 00EX393), vol. 5, pp. 3385–3388. Hefei, China (2000). https://doi.org/10.1109/WCICA.2000.863164
18. Mathew, N.J., Rao, K.K., Sivakumarn, N.: Swing up and stabilization control of a rotary inverted pendulum. In: IFAC International Symposium on Dynamics and Control of Process Systems, The International Federation of Automatic Control, Mumbai (2013)

How to cite this article: Pramanik, S., Anwar, S.: Robust controller design for rotary inverted pendulum using $H\infty$ and μ-synthesis techniques. J. Eng. 2022, 249–260 (2022). https://doi.org/10.1049/tje2.12078